Composite Structures 387 (2026) 120282

Contents lists available at ScienceDirect

Composite Structures

journal homepage: www.elsevier.com/locate/compstruct

Experimental study on the thermal-dependent nonlinear dynamics of a bi-metallic beam

Moslem Molaie [a], Antonio Zippo [a], Emil Manoach [b], Simona Doneva [b], Jerzy Warminski [c], Francesco Pellicano [a,*]

[a] Department of Engineering "Enzo Ferrari", University of Modena and Reggio Emilia, Modena, Italy
[b] Institute of Mechanics, Bulgarian Academy of Sciences, Sofia, Bulgaria
[c] Department of Applied Mechanics, Lublin University of Technology, Lublin, Poland

ARTICLE INFO

Keywords:
Post-buckling dynamics
Pre-buckling dynamics
Thermo-mechanical effect
Bi-metallic beam
Experimental modal analysis
Nonlinear vibration
Stability

ABSTRACT

This study investigates the nonlinear dynamics of a bi-metallic beam composed of aluminum alloy and copper layers joined through an explosive welding technique, with emphasis on the effect of temperature on its stability and vibrational characteristics. Although thermal buckling and vibration of the beams have been extensively investigated through analytical and numerical methods, experimental studies capturing the combined effects of thermal loading, material heterogeneity, geometric nonlinearity, and damping evolution across buckling are still scarce. To address this gap, various experimental tests—impact, random control, and stepped-sine—are conducted to investigate the dynamics of the system. Experimental vibration tests were performed within a climate chamber, where the bi-metallic beam was excited at its base using a shaking table to evaluate large-amplitude vibrations across a temperature range from 5°C to 70°C. The results reveal a pronounced non-monotonic evolution of the fundamental frequency, decreasing by nearly 32% as the temperature approaches the critical buckling temperature at about 30°C, followed by a significant recovery in the post-buckling regime. The damping ratio exhibits an inverse trend, peaking at approximately 3.5% at 35°C. The uniform aluminum beam tested under different thermal conditions conducted to delve into the dynamics of the bi-metallic beam. At the buckling threshold, the dynamic frequency–response curves display a softening-to-hardening transition. The results contribute new insights into the thermal dependence of nonlinear vibrations in layered metallic structures, offering valuable guidelines for the design, reliability, and performance optimization of thermally loaded components.

1. Introduction

Advances in modern engineering have increasingly relied on multi-material and layered components to achieve enhanced structural performance, enabling more efficient and tailored design solutions such as weight reduction and improved functionality [1,2]. Bi-metallic systems—combining materials with distinct mechanical and thermal properties—offer significant functional advantages but also introduce complex behaviors that must be thoroughly understood to ensure reliability, especially under varying environmental conditions. In particular, predicting the dynamic response of such structures requires careful consideration of both their static and dynamic characteristics.

Research on the vibrational behavior of beams has a long and established history [3]. In 1973, Rehelfield [4] studied nonlinear free vibration of beams applying a perturbation technique. Bennouna et al. [5] investigated the variation of the fundamental mode due to nonlinearity of a clamped–clamped uniform beam through a numerical model. Benamar et al. [6] proposed a general model for large vibration amplitudes of thin straight beams. Pellicano et al. [7] investigated the nonlinear vibration of a simply supported beam resting on a nonlinear cubic spring bed. The dynamics of an axially moving beam was investigated by Pellicano [7–9] using a multi-modal approach and a Galerkin procedure. The multi-layered beams are also used in the fluid-conveying spatial-pipe systems presented for example in Ref. [10]. The proposed nonlinear mechanical model for single and double clamp assemblies effectively captured softening effect and energy dissipation in the

* Corresponding author.
E-mail addresses: moslem_molaie@unimore.it (M. Molaie), antonio.zippo@unimore.it (A. Zippo), e.manoach@imbm.bas.bg (E. Manoach), s.doneva@imbm.bas.bg (S. Doneva), j.warminski@pollub.pl (J. Warminski), francesco.pellicano@unimore.it (F. Pellicano).

https://doi.org/10.1016/j.compstruct.2026.120282
Received 2 December 2025; Received in revised form 19 February 2026; Accepted 21 March 2026
Available online 26 March 2026

clamps. The influence of nonlinear effects of materials, clamps and fluid parameters on the natural characteristics have been there demonstrated.

Functionally graded structures like beams, shells, and plates find application in different fields like Aerospace, Naval, Biomedical, Nuclear, Energy, Civil engineering. The influence of material variation on the buckling load induced by thermal fields in an Euler–Bernoulli beam composed of two-directional functionally graded materials was studied in [11–13]. Tahir et al. [14] examined how moisture and temperature influence wave propagation in porous functionally graded (FG) sandwich plates, as well as the material expansion. Arshid et al. [15] analyzed the dynamics of a three-layer sandwich microplate supported by a Pasternak foundation, the microplate was composed of a porous FG core and piezoelectric nanocomposite face sheets, the system was excited by an electric field. Malekzadeh et al. [16] used a first-order shear deformation theory for investigating the dynamics of an FG beam subjected to a two-dimensional thermal field.

The relationship between the degradation of natural frequencies and the approach to a critical buckling condition has been extensively studied and forms the theoretical basis of the Vibration Correlation Technique (VCT), a non-destructive method for estimating buckling loads in slender and thin-walled structures. Early formulations of VCT demonstrated that, for ideal beams and columns, the square of the natural frequency decreases approximately linearly with increasing compressive load, vanishing at the critical buckling point [17]. Building on this concept, VCT has been successfully applied to a wide range of thin-walled structures, particularly cylindrical shells and panels, with numerous experimental and numerical studies reported in the aerospace field [18,19]. Extensive investigations conducted by DLR (German Aerospace Center), and collaborating institutions have demonstrated the capability of VCT to predict buckling loads without reaching structural collapse, even in the presence of geometric imperfections and complex boundary conditions [20–22]. Nevertheless, it has also been shown that the classical VCT framework is primarily intended for critical load identification in the pre-buckling regime and is typically formulated within a linear or weakly nonlinear vibration context. For imperfection-sensitive structures, deviations from the ideal linear frequency–load relationship are frequently observed as the buckling load is approached, requiring modified or empirical correlation schemes [19,20,22]. Moreover, VCT-based studies are primarily aimed at correlating the monotonic degradation of natural frequencies in the pre-buckling regime with the critical buckling load and are not intended to investigate the dynamic response beyond instability. For imperfection-sensitive structures, it has been shown that deviations from the ideal linear frequency–load relationship occur as the buckling load is approached, requiring modified or empirical VCT formulations.

Classical thermal stress models for bi-material beams provide a well-established theoretical framework for estimating thermally induced curvature, axial force, and static buckling conditions in layered beams subjected to uniform temperature variations [23,24]. These models successfully capture the role of differential thermal expansion, elastic mismatch, and geometric constraints in determining the critical buckling temperature and the associated equilibrium configuration under idealized assumptions. However, they are primarily formulated within a quasi-static framework, rather than on the evolution of the dynamic response [25,26]. From a dynamical systems perspective, the thermal buckling of an ideal, perfectly symmetric beam is expected to occur through a pitchfork bifurcation, characterized by the vanishing of the fundamental natural frequency at the critical temperature and the emergence of two symmetric post-buckled equilibria. In practical bi-metallic beams, however, symmetry is broken by material heterogeneity, through-thickness stiffness asymmetry, differential thermal expansion, and different layer thickness. Under these conditions, bifurcation theory predicts that the ideal pitchfork is generically unfolded into an imperfect bifurcation characterized by saddle-node (fold) points rather than symmetric branching. As a consequence, the natural frequency does not necessarily vanish at the critical temperature but instead reaches a rounded minimum and subsequently recovers in the post-buckled regime, often accompanied by hysteresis and jump phenomena under parameter variation [26]. This imperfect-bifurcation scenario provides a consistent physical interpretation for the experimentally observed non-monotonic frequency evolution, and post-buckling frequency recovery, in thermally loaded bi-metallic beams, thereby extending classical thermal stress models beyond their idealized assumptions.

Beams consisting of two layers of different materials and thicknesses are special cases of composite structures. Bi-material Euler–Bernoulli beams with longitudinal and inverted cracks were studied by an analytical method based on frequency measurements in [27]. Most research on the thermomechanical behavior of the bi-material beams is devoted to static applications [28–30]. One of the earliest studies on the bending of bi-material beams can be found in Ref. [31]. Other studies such as Refs. [32–35] investigated the thermal and mechanical behavior of bi-metallic beams. In Ref. [36] the combination of thermal and oscillating magnetic fields applied on a beam was analyzed using the Hamilton principle and the Euler–Bernoulli theory. The effect of elevated temperature on the coupled vibrations of bi-material beams subjected to mechanical and thermal loads was studied numerically in [37]. To develop the theoretical model, the geometrically nonlinear version of the Timoshenko beam theory was applied. The governing equations of the bi-material beam were derived by applying the geometrical, constitutive, and equilibrium equations of each layer. Later, this model was extended and based on 3-mode reduction, modal interactions, and instability zones were evaluated [38]. The reduced model was compared with results based on modal experimental analysis and the finite element method, and a very good agreement was found. Doneva et al. [39] examine the nonlinear dynamic behavior of a bilayer (two-layered) composite beam made of materials of different thicknesses under combined mechanical and thermal loading. They consider two types of thermal loading: (i) uniform temperature across the whole beam, and (ii) a linear temperature gradient through the thickness. The authors build reduced-order dynamic models using the first three normal modes of the beam, and also derive a one-mode reduction model which is then solved via the Harmonic Balance Method. Recent studies have devoted significant attention to the nonlinear vibration, buckling, and post-buckling behavior of beam structures. Eltaher et al. [40] in 2019, analyzed the nonlinear vibration and post-buckling behavior of imperfect beams resting on nonlinear elastic foundations. Their study highlighted how different imperfection modes, both periodic and non-periodic, significantly affect critical buckling loads, post-buckling responses, and vibration frequencies. Dong et al. [41] developed an analytical formulation to investigate the buckling, post-buckling, and vibration behavior of micro-scale laminated composite beams under hygrothermal environments. By incorporating temperature- and moisture-dependent material properties into a modified couple stress theory, the study captured both size effects and nonlinear responses. The results revealed that variations in temperature and hygroscopic concentration significantly reduce the critical buckling load and alter the post-buckling configuration and vibration frequencies. Emam et al. [42] investigated the post-buckling and free vibration behavior of geometrically imperfect, multilayer nanobeams subjected to pre-stress load, using the Eringen nonlocal elasticity model combined with nonlinear Euler-Bernoulli beam theory. They examined how three parameters — imperfection amplitude, small-size (nonlocal) parameter, and lamination layout — affect the buckling load, post-buckled deflections, and the natural frequencies for the first several vibration modes, both in pre-buckling and post-buckling regimes. In 2022, Daneshkhah et al. [43], used a refined structural and nonlinear theory to investigate the free vibration and post-buckling response of thin-walled beams and flexible plate structures. Pagani et al. [44] investigate how the vibration modes of compact and thin-walled metallic beams change when the beams undergo large deflections and post-buckling deformations. They use refined beam models within the Carrera Unified Formulation (CUF)

framework to capture geometrical nonlinearity and cross-section deformations, and they examine how mode shapes and natural frequencies evolve beyond the linear regime. Their results show that certain modes shift or "jump" as deflection grows, and that warping and cross-sectional effects become more important when the beam is thin-walled or under large displacements.

Understanding how the thermal load influences the stability and vibration behavior of composite structures has become an increasingly important topic in modern structural dynamics, as temperature-dependent stiffness and geometric nonlinearity can profoundly alter system behavior. Recent investigations by Chakraborty et al. [45] have highlighted the influence of thermal gradients on the stability and dynamic response of composite and multi-material structures. Chakraborty et al. [45] demonstrated that bi-directional functionally graded composite plates subjected to non-uniform temperature gradients experience significant alterations in both thermal post-buckling behavior and vibration characteristics, emphasizing the sensitivity of dynamic performance to spatial variations in thermal loading. Under localized heating, composite plates reinforced with randomly distributed CNTs were shown to undergo earlier thermal post-buckling and pronounced frequency shifts, as quantified in their nonlinear plate analyses [46]. In 2019, Chakraborty et al. [47] analyzed laminated cylindrical shell panels incorporating CNT-reinforced functionally graded layers and found that material heterogeneity and geometric curvature strongly enhance both buckling thresholds and natural frequencies. Extending these insights to beam-like structures, Chakraborty et al. [48] reported that CNT-reinforced composite beams under combined thermo-mechanical loading exhibit substantial shifts in buckling loads and nonlinear equilibrium paths when temperature-dependent material properties and reinforcement agglomeration are considered. Dash et al. [49] investigated CNT-reinforced composite beams under coupled thermo-mechanical loading and found that the support conditions can significantly affect the vibrational beam characteristics. Besides, Dash and Dey [50] developed a semi-analytical framework for variable-stiffness laminated composite beams, revealing that both spatial stiffness variation and thermal effects critically affect post-buckling vibration behavior.

In the present investigation, the thermo-mechanical dynamic behavior of a bi-metallic beam composed of aluminum and copper layers is investigated. While thermal buckling and vibration of beams have been widely studied using analytical and numerical approaches, experimental evidence capturing the coupled effects of thermal loading, material heterogeneity, geometric nonlinearity, and damping evolution across buckling remains limited. To address this gap, a series of impact, random, and stepped-sine excitation tests are performed under controlled thermal conditions inside a climate chamber, with the beam subjected to base excitation over a temperature range from 5°C to 70°C. It is worthwhile to notice that within the investigated range, the variations in elastic modulus and thermal expansion coefficient are negligible, indeed, both the elastic modulus, the Poisson ratio and the thermal expansion coefficient vary 1–2% in the temperature interval 5-70°C [51,52]. Note that, the investigated temperature range was selected, without targeting specific application, to ensure controlled experimental conditions, material stability, and repeatable measurements while enabling clear observation of thermo-mechanically induced nonlinear dynamic phenomena. To conduct this study, the term "thermal-dependent" is used to denote the influence of thermally induced stresses on the nonlinear dynamic behavior, which are also affected by indirect geometric effects arising from constrained thermal expansion, rather than by temperature-dependent degradation of material properties. The study aims to explore how operational temperature variations affect the fundamental vibration characteristics and stability of such multi-material systems, where the interaction between thermal loading, and geometric nonlinearity plays a decisive role. Indeed, comprehensive experiments are carried out under precisely controlled thermal conditions within a climate chamber. The bi-metallic beam is mounted on an electrodynamic shaker and subjected to base excitation to characterize its dynamic response across a wide temperature range. Moreover, to have better sight, the dynamics of the bi-metallic beam is compared with the dynamic response of uniform Aluminum beam. The main objective is to establish a detailed understanding of the thermal-dependent dynamic response of bi-metallic structures, offering a foundation for their optimized design and reliable operation in thermally variable environments.

2. Experimental setup

The considered bi-metallic beam is made of two layers of metals: aluminum alloy *Al* 1050 (material 1 — bottom layer) and copper *C* 12,500 (material 2 — upper layer). Fig. 1 shows the geometry of the bi-metallic beam, the dimensions as well as the material parameters of the layers. The aluminum–copper beam investigated in this study was manufactured by explosion welding, using a detonation velocity of 2000 m/s and an impact velocity of 265 m/s. Following the welding process, residual stresses were relieved by heat treating the finished bi-metallic beam at 300°C for 30 min, followed by air cooling. This treatment corresponds to annealing for aluminum and semi-annealing for copper and is known to significantly reduce residual stresses introduced during explosive welding. The interface microstructure was subsequently examined to verify the absence of intermetallic compound formation. In addition, tensile testing of the bi-metallic strip confirmed that interfacial delamination does not occur, even at failure, indicating a robust metallurgical bond between the layers [53–55].

In this analysis, the beam is clamped at both ends, as they represent a practical configuration from an experimental standpoint and allow for a clear assessment of the effects of thermal loads; this means that both axial and transversal displacement, as well as rotations, are locked at the boundaries. To implement these conditions, the beam is mounted on an aluminum Vibration Table Adapter (VAT), which serves as the interface between the beam and the shaker. The ends of the beam are secured using two steel plates and fastened with M12 bolts, ensuring a rigid connection. All bolts are tightened uniformly to a torque of 40 Nm in order to guarantee consistency and repeatability of the boundary conditions. The overall setup, including the VAT and fastening system, is shown in Fig. 2. In Fig. 3, the detail of the physical realization of the clamping is shown, two steel blocks present a groove having the width of the beam and a total depth (summation of the two grooves) 0.2 mm less than the beam thickness; this guarantee that: i) when the two blocks are mounted on the fixture, the bolts exert a force which completely locks the beam end; ii) the bolts cannot deform the beam end more than 0.2 mm, so the plastic deformation is limited and the probability of fatigue cracks at the boundaries during the vibration tests is limited; iii) moreover, a chamfer is applied on the block to avoid edge effects and further reduce the probability of failure.

A Dongling ET-40-370 electrodynamic shaker is used to apply a seismic base motion to the structure, which induces an inertial excitation. The shaker can deliver a peak force of 40 kN, with a maximum acceleration of 100 g, it can carry a static payload having a mass of 500 kg, the operational frequency band ranges from 1 to 2800 Hz. In the experimental setup, the shaker provides the base motion that indirectly excites the system through the beam rigid body inertia of the beam itself, enabling an investigation of its dynamic response. The electrodynamic shaker is closed loop controlled by a Siemens LMS SCADAS MOBILE with TestLab software. To evaluate the influence of environmental conditions, the shaker is integrated with a climatic chamber that allows tests to be conducted under controlled thermo-hygrometric environments. Importantly, the climatic chamber frame is designed to remain structurally independent from the shaker frame, thus avoiding any unwanted mechanical coupling effects. The response of the beam under excitation is measured using a Polytec OFV-505 laser vibrometer, featuring a displacement resolution of 0.1 pm, a velocity range up to ± 25 m/s, and a frequency bandwidth of 0–24 MHz. This non-contact measurement technology is particularly advantageous as it eliminates

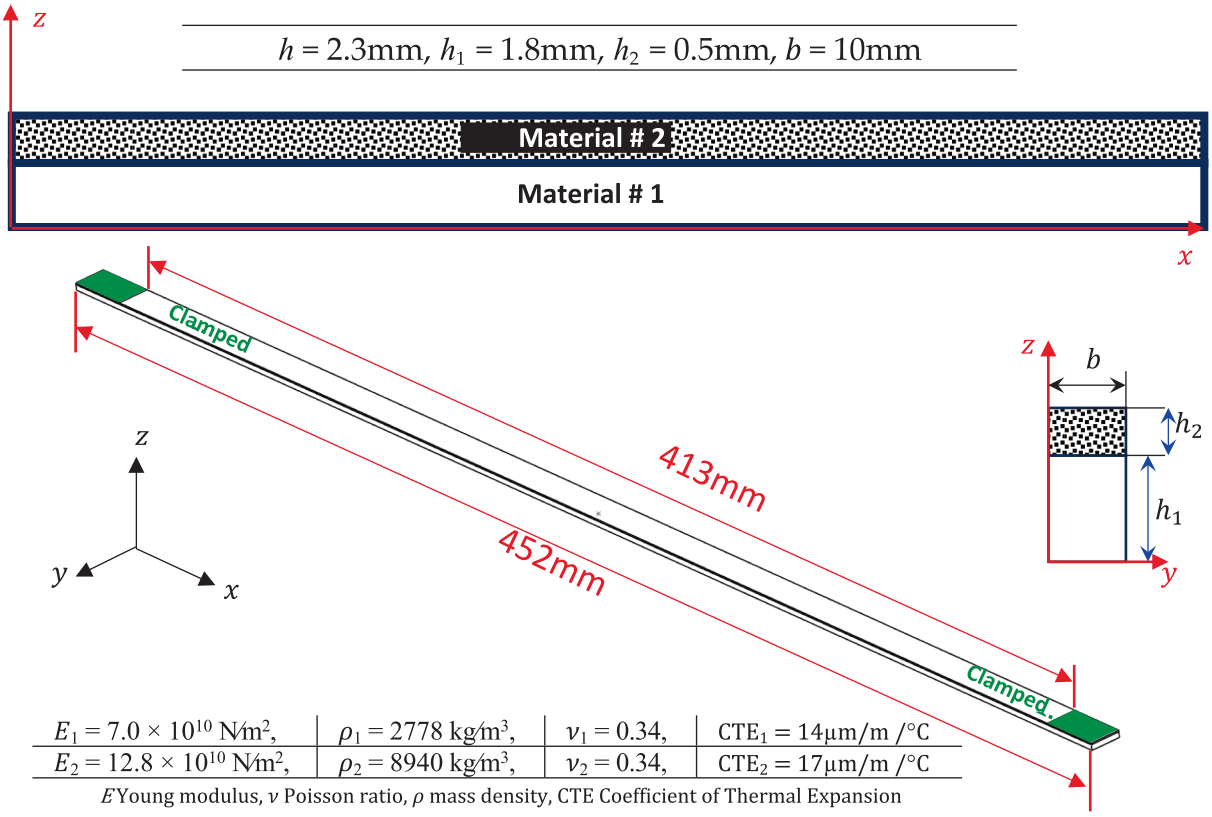

$E_1 = 7.0 \times 10^{10}$ N/m^2,	$\rho_1 = 2778$ kg/m^3,	$\nu_1 = 0.34$,	$CTE_1 = 14\mu m/m/°C$
$E_2 = 12.8 \times 10^{10}$ N/m^2,	$\rho_2 = 8940$ kg/m^3,	$\nu_2 = 0.34$,	$CTE_2 = 17\mu m/m/°C$

E Young modulus, ν Poisson ratio, ρ mass density, CTE Coefficient of Thermal Expansion

Fig. 1. Geometry of the beam.

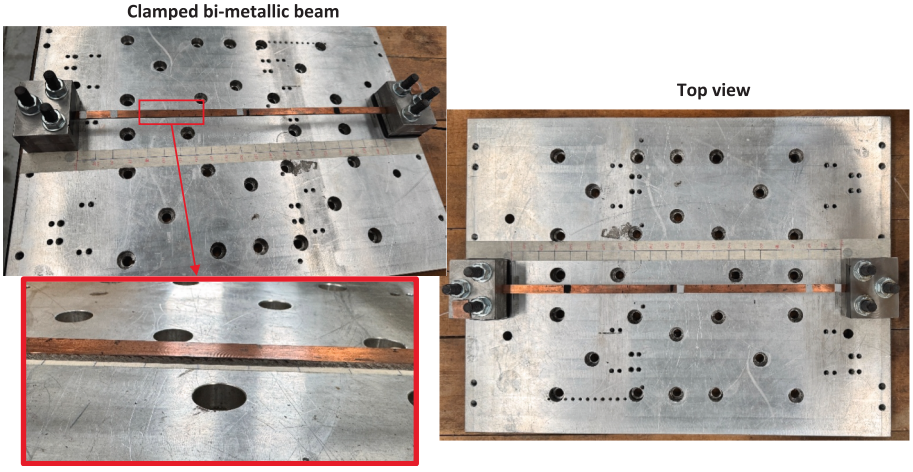

Fig. 2. Implementing the clamped condition.

the influence perturbations, such as added masses, ensuring that the intrinsic behavior of the specimen is preserved. The vibrometer is considered to measure the lateral velocity of the beam at a reference location positioned 200 mm from one of the edges. Moreover, because of the high operating temperatures during the experimental test, it is not possible to place the vibrometer head inside the chamber. To overcome

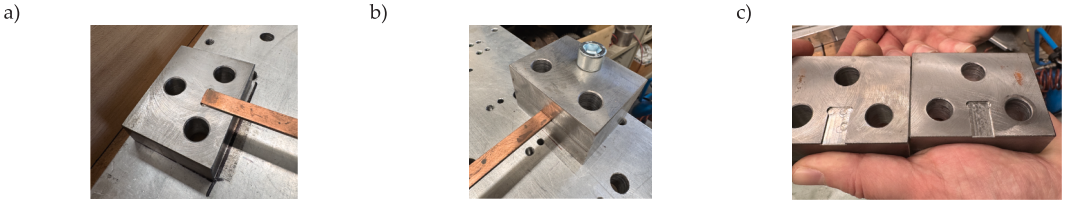

Fig. 3. Mechanical detail of the clamping.

this issue, a mirror system (periscope) is implemented to redirect the laser beam onto the lateral surface of the beam, as illustrated in Fig. 4. For non-contact displacement measurements, a Micro-Epsilon optoNCDT 2300 laser triangulation sensor is used. The sensor covers measuring ranges of 100 mm. In order to control the displacement of the shaker base, a mono-axial accelerometer with 192 mv/s sensitivity is placed on one of the supports. The axial forcing load of the vibrating base is applied with an open-loop control strategy; this has been made on purpose to avoid interference with nonlinear phenomena that could appear during the tests; a real-time closed-loop control has been used on the generated voltage signal sent to the shaker amplifier.

3. Experimental results

The experimental campaign consists of two sections: i) a traditional modal testing having the purpose of identifying the linear properties of the beam, namely, natural frequencies, damping ratios and modal shapes; ii) nonlinear dynamic analysis, harmonic excitation, to investigate large amplitude of vibration in resonance conditions. For the test i) a Random control method is considered, i.e. a low energy broad band-controlled excitation; for the test ii) a Stepped Sine control is used, indeed, in this case we are interested in the periodic or non-periodic responses to a harmonic forcing. Both tests i) and ii) are carried out at different temperatures, in order to evaluate the thermal sensitivity of the system at low and large amplitude of vibration. For analyzing the nonlinear dynamic scenario, the Stepped Sine technique is considered to examine the dynamic response of the system in a controlled manner, enabling precise evaluation of resonances and dynamics of the bi-material beam.

3.1. Modal testing, impact analysis

Impact modal analysis was performed to identify the mode shapes of the beam at 21°C. A micro-hammer with a vinyl tip and a laser were used to excite the structure and measure the response, respectively. Specifically, a grid of 22 points was defined on the beam, and a roving hammer method was employed to obtain the first three mode shapes and their corresponding natural frequencies. The measured results are presented in Table 1 and relative mode shapes in Fig. 5.

3.2. Modal testing, base random excitation

The random vibration control is imposed on the base with the aim of exciting the first three modes of vibration of the beam. The test is conducted in a broadband random excitation with a root-mean-square (RMS) level of 0.5 g over a frequency range of 25 Hz to 800 Hz, with a resolution of 1 Hz. The reference profile in the form of Power Spectral Density (PSD) for the random control test is defined in Fig. 6. The reference PSD curve was a constant flat line: 0.000322581 g^2/Hz, with upper/lower alarm band of 3 dB (alarm thresholds are shown in orange in Fig. 6) and upper/lower abort band of 6 dB (abort thresholds are shown in red in Fig. 6). This type of excitation allowed us to identify all modes within the frequency range of interest. The beam was placed inside a climate chamber to systematically vary the temperature from 5°C to 70°C, this allows to determine how the thermal conditions affect the natural frequencies and the damping ratios. A standard FRF-based approach was used in experimental tests. The experimental FRFs are obtained from time histories using H2 estimator based on power and cross-spectral densities. The FRFs are then post-processed using the "curve fitting" algorithm available in the Siemens-TestLab, the Polymax algorithm, which allows identifying the natural frequencies and the damping ratios as well as modal shapes if a suitable number of points are measured on the structure.

A preliminary analysis of the experimental setup is needed to check if the fixture is stiff enough to avoid interactions with the specimen (the beam), indeed, such interactions can affect the specimen response and introduce spurious dynamics. The modal analysis of the VTA reveals that its first natural frequency is located at 735 Hz, which lies within the frequency range of interest, highlighting the need for careful response monitoring in this region to avoid undesirable modal coupling between the VTA and the test specimen.

Figs. 7 and 8 represent the FRF of the beam at different temperatures.

Table 1
Damping and natural frequencies of the beam obtained from impact test 21°C.

Mode	Natural frequency [Hz]	Damping [%]
1 – Fig. 5.a	56.9	0.17
2 – Fig. 5.b	163	0.16
3 – Fig. 5.c	339.8	0.18

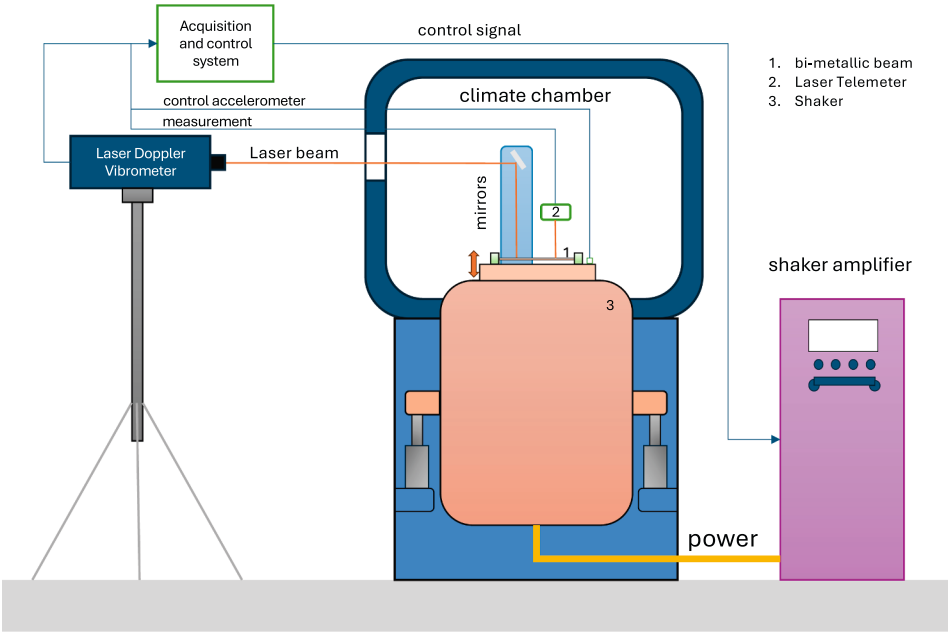

Fig. 4. Detailed schematic of the setup test with the equipment.

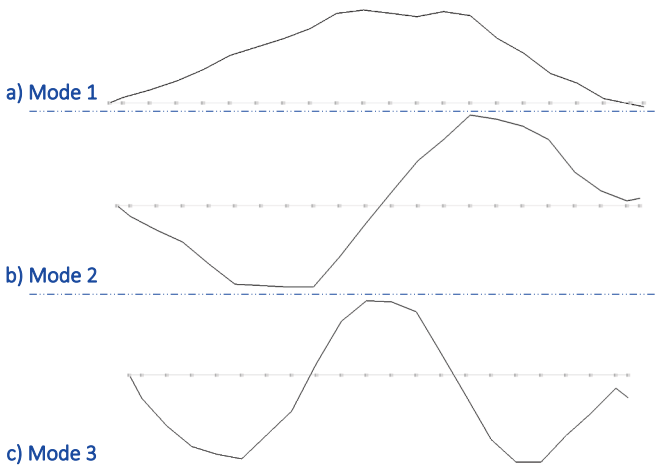

Fig. 5. Measured mode shapes obtained from impact test on bi-metallic beam.

Both figures show the FRFs, and the reason they are separated is to show the "turning point" that occurred around 30°C, i.e. the temperature for which the trend of the fundamental damping and frequency is inverted due to the onset of static buckling. From the presented results, it is obvious that by increasing the temperature, the first natural frequency of the system is reduced, see Fig. 7, until a critical temperature, from that temperature on, increasing the temperature the fundamental frequency increases, see Fig. 8. Such behavior depends by the axial stress generated in the beam. We set up the tests at room temperature (27°C); for lower temperature the thermal expansion of the beam is negative (shortening of the specimen) inducing tension and increasing the stiffness; for higher temperature the expansion induces axial compression, and, due to the extreme slenderness of the beam, it immediately buckles.

The beam experiences two distinct states: the pre-buckling and post-buckling states. This behavior is confirmed by examining the results presented in Fig. 9 and Table 2. An additional element to consider is the bi-metallic nature of the beam; when a bilayer beam made of Aluminum and Copper is clamped at both ends and is subjected to a uniform temperature variation, its vibrational behavior is strongly influenced by thermal effects. As the temperature rises, the difference in thermal expansion between the two materials induces internal stresses and slight bending, while the clamped ends prevent free expansion. This leads to a tensile/compressive axial load along the beam, which effect is to increase/reduce its stiffness. Consequently, the first natural frequency gradually decreases as the temperature approaches the critical point (buckling), reflecting a softening of the structure. Near the critical temperature, the beam undergoes buckling; however, in this problem the fundamental frequency does not approach zero at the buckling point, because of the dissymmetry due to the different thermal expansions of the two layers, which transforms the pitchfork bifurcation of a perfect uniform beam into a saddle node bifurcation (see Refs. [56–59]). This explains why in Fig. 9 the first natural frequency does not drop exactly to zero, but it reaches a minimum in correspondence with the buckling. Indeed, this minimum frequency would collapse to zero only in the case of a perfectly symmetric and homogeneous beam [26], whereas in the present bi-metallic configuration material asymmetry prevents a zero-frequency condition at buckling. After buckling, the beam adopts a new equilibrium configuration with a curved shape. The geometric curvature introduces additional stiffness, causing the first natural frequency to increase again as the temperature continues to rise. The first natural frequency exhibits non-monotonic behavior: it decreases before

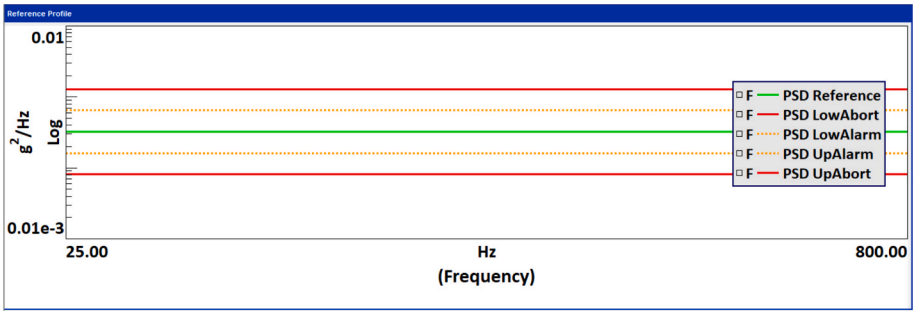

Fig. 6. Reference profile used to conduct the random control test.

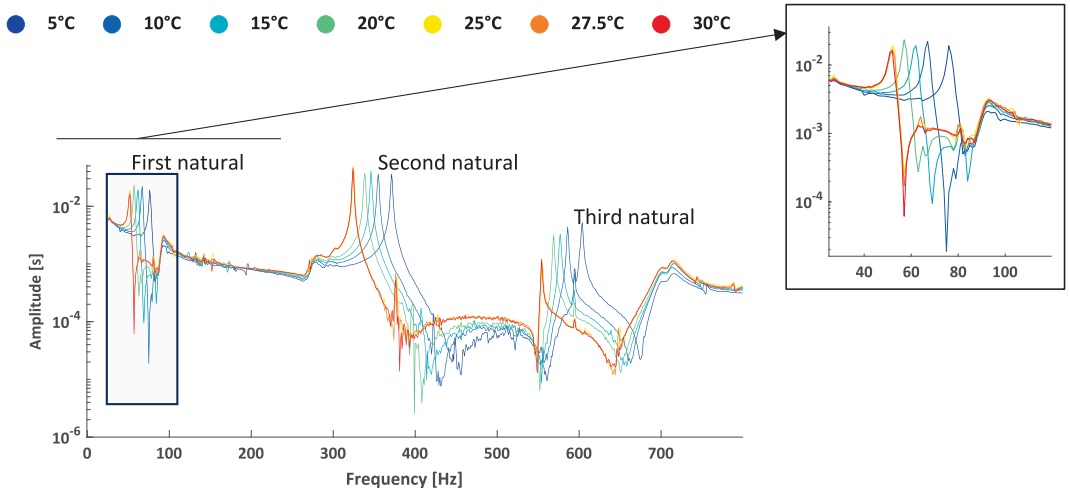

Fig. 7. FRF diagram regarding temperature from 5°C to 30°C (bi-metallic beam).

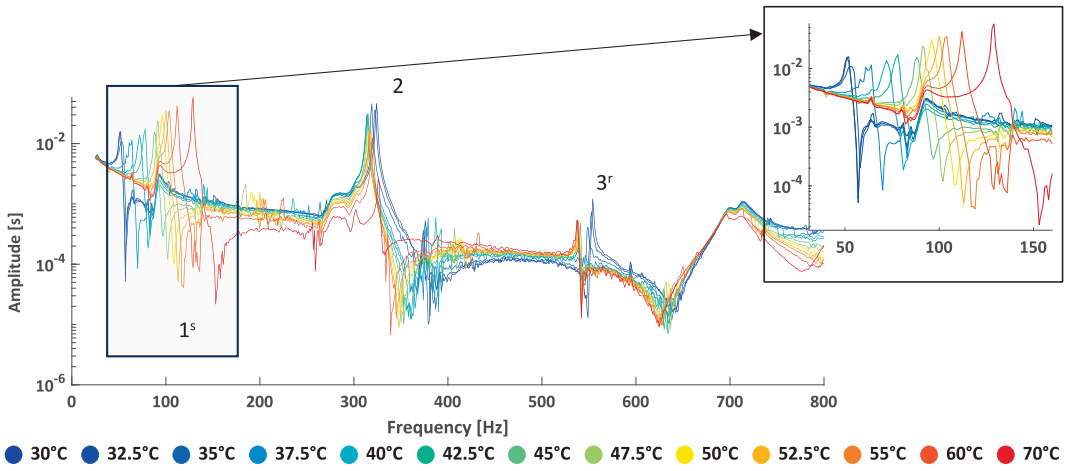

Fig. 8. FRF diagram regarding temperature from 30°C to 70°C (bi-metallic beam).

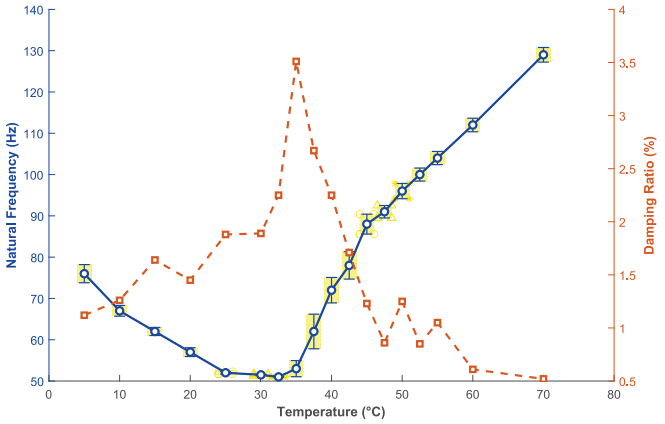

Fig. 9. First natural frequency and damping ratio of the bi-metallic beam under different temperatures.

buckling due to thermal softening caused by the reduction of tension and the following compression, it reaches a minimum near the critical temperature, and then increases after buckling as a result of the geometric stiffening in the post-buckled configuration. This behavior is particularly pronounced in bilayer beams due to the combined effects of material mismatch, thermal expansion differences, and nonlinear post-buckling deformation. Moreover, in Fig. 9, the tolerance range has been indicated for the blue curve at the points corresponding to the natural frequency values measured at different temperatures. The climatic chamber features a temperature control tolerance of ±1°C, which results in varying tolerance margins for the natural frequency values at each temperature, as reported in Table 2.

The same analysis is carried out on the uniform aluminum beam. Fig. 10 shows the temperature dependence of the first natural frequency f_n and the modal damping ratio ξ for a clamped–clamped uniform aluminum beam. The frequency exhibits a reduction from 95 Hz at −10°C to a minimum of 71 Hz at 5°C, and subsequently an increment to 104 Hz at 25°C Table 3. This behavior arises from the competition between the temperature dependence of the elastic modulus—which tends to reduce f_n as temperature increases—and the thermally induced axial force generated by the restrained thermal strain at the clamped ends. At the assembly temperature, the beam is stress-free, below such temperature the beam is subjected to axial tension, which stiffens the structure and increases f_n; above the assembly temperature the beam experiences axial compression, which softens the response and reduces the natural frequencies. The observed minimum of the fundamental frequency near 5°C is consistent with the transition between tensile and compressive axial states and a balance between modulus softening and axial-load effects. The damping ratio reaches a maximum of 1.3% in the vicinity of this transition, whereas ξ is lower (0.7–0.9%) at both colder and warmer temperatures, where the axial state is well away from the crossover.

Fig. 11 compares the thermal-dependent evolution of the normalized natural frequency for the uniform aluminum and bi-metallic (Al–Cu) beams. Both configurations exhibit a characteristic U-shaped trend, with a minimum near the critical temperature of 5°C for the uniform Al beam and 30°C for the bi-metallic beam, corresponding to the transition from tensile to compressive thermal stress. In the pre-buckling region (highlighted in yellow, Fig. 11-a), the frequency decreases almost linearly with temperature, with slopes of approximately –0.6 for the aluminum and –0.7 for the bi-metallic beam, indicating a gradual stiffness

Table 2
The variation of the beam damping ratio and natural frequencies corresponding to the first mode (bi-metallic beam).

Temperature [°C]	**5 [±1°C]**	**10 [±1°C]**	**15 [±1°C]**	**20 [±1°C]**	**25 [±1°C]**	**30 [±1°C]**	**32.5 [±1°C]**	**35 [±1°C]**	**37.5 [±1°C]**
Lowest tol. range	73.8	65.71	61.02	55.93	51.69	51.33	50.88	51.05	57.81
f_n [Hz]	**76**	**67**	**62**	**57**	**52**	**51.5**	**51**	**53**	**62**
Highest tol. range	78.2	68.29	62.98	58.07	52.31	51.67	51.12	54.95	66.19
ξ [%]	**1.12**	**1.26**	**1.64**	**1.45**	**1.88**	**1.89**	**2.25**	**3.51**	**2.67**

Temperature [°C]	**40 [±1°C]**	**42.5 [±1°C]**	**45 [±1°C]**	**47.5 [±1°C]**	**50 [±1°C]**	**52.5 [±1°C]**	**55 [±1°C]**	**60 [±1°C]**	**70 [±1°C]**
Lowest tol. range	68.92	74.69	85.59	89.49	94.15	98.42	102.4	110.36	127.23
f_n [Hz]	**72**	**78**	**88**	**91**	**96**	**100**	**104**	**112**	**129**
Highest tol. range	75.08	81.31	90.41	92.51	97.85	101.58	105.6	113.64	130.77
ξ [%]	**2.25**	**1.71**	**1.23**	**0.86**	**1.25**	**0.85**	**1.05**	**0.61**	**0.52**

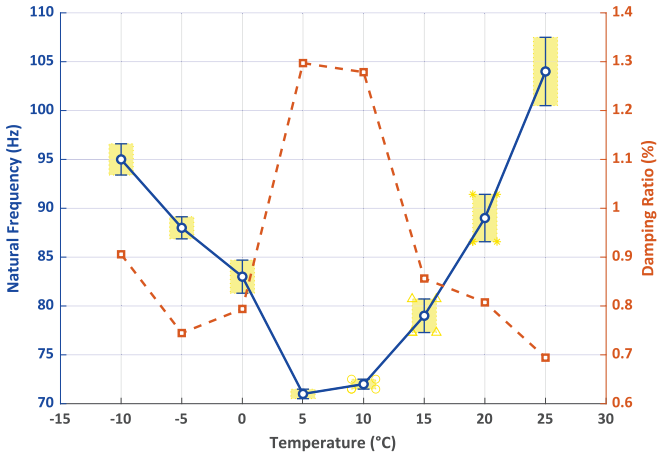

Fig. 10. First natural frequency and damping ratio of the uniform Al beam under different temperatures.

reduction due to thermal softening and the buildup of compressive stress. The bi-metallic beam shows a slightly steeper decline, reflecting its higher sensitivity to thermal expansion mismatch between the aluminum and copper layers. Beyond the critical temperature (green region, Fig. 11-b), both specimens exhibit a recovery in frequency associated with geometric stiffening in the post-buckled configuration. The slope of the frequency increase, however, is significantly larger for the bi-metallic beam (≈ 1.7) compared with the uniform aluminum one (≈ 0.9), demonstrating that the interaction between material heterogeneity and residual thermal curvature enhances the post-buckling stiffness. Consequently, while the uniform beam responds primarily to uniform thermal stress and elastic-modulus variation, the bi-metallic system displays a more pronounced nonlinear behavior, governed by thermally induced bending.

3.3. *Nonlinear vibrations in pre- and post-buckling*

The third experimental campaign is performed using the Stepped Sine approach, in which the system is excited with a pure sine wave at discrete frequencies, holding each frequency for a sufficient number of cycles before advancing to the next. The excitation frequency range was selected to ensure that the fundamental resonance was included, namely between 20 Hz and 90 Hz, note that in this range of frequencies no interaction with the fixture is expected. To allow comparison across tests, the results were normalized with respect to the first natural frequency of the beam at each temperature. The experiments were

Table 3
The variation of the beam damping ratio and natural frequencies corresponding to the first mode (uniform Al beam beam).

Temperature [°C]	−10 [±1°C]	−5 [±1°C]	0 [±1°C]	5 [±1°C]	10 [±1°C]	15 [±1°C]	20 [±1°C]	25 [±1°C]
Lowest tol. range	93.40	86.87	81.31	70.51	71.49	77.28	86.58	100.50
f_n [Hz]	**95**	**88**	**83**	**71**	**72**	**79**	**89**	**104**
Highest tol. range	96.60	89.13	84.69	71.49	72.51	80.72	91.42	107.50
ξ [%]	**0.91**	**0.74**	**0.79**	**1.30**	**1.28**	**0.86**	**0.81**	**0.69**

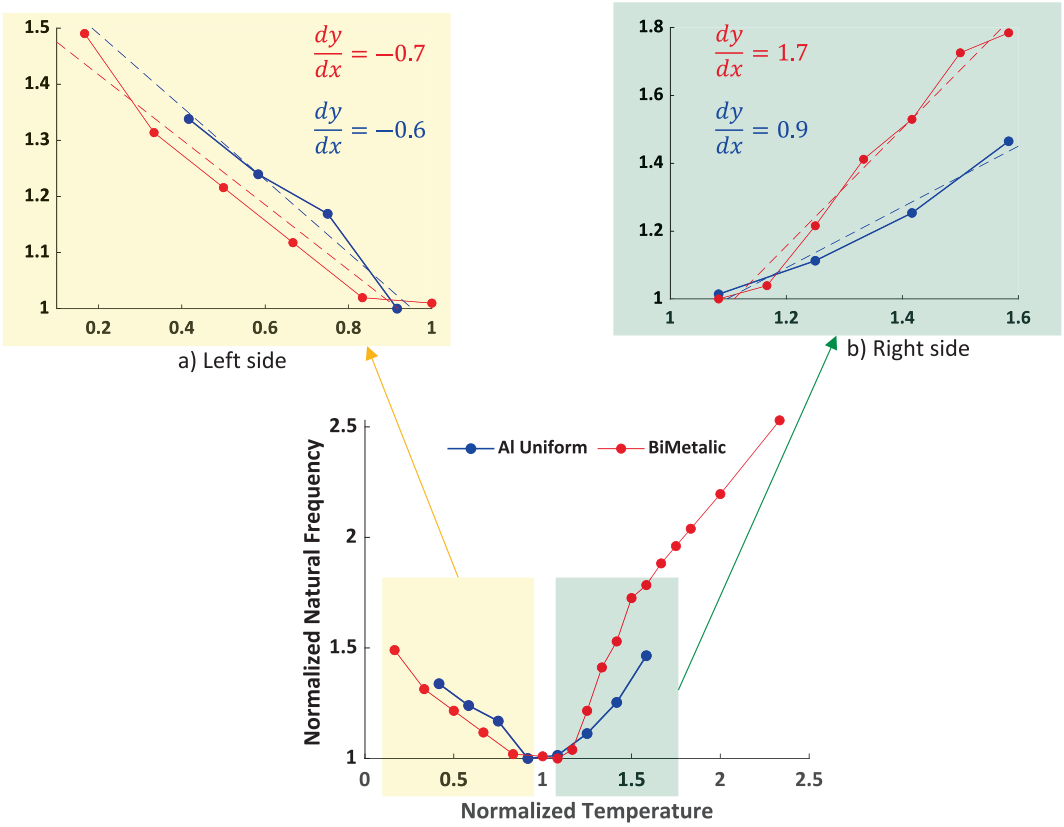

Fig. 11. Natural frequency comparision between Bi-metallic and uniform Aluminum beams.

conducted in both forward and backward frequency sweeps to capture possible nonlinear responses, as shown in Fig. 12. In this context, forward test sweep from low to high excitation frequency, while backward test sweep from high to low frequency. This test procedure can better reveal the softening/hardening dynamic behaviors of the specimen under test and can be applied both for experimental or numerical analysis. Fig. 12(a) shows the displacement measured by the laser telemeter for a case in the post-buckling state at 37.5°C, where the excitation step size was 0.1 Hz, with 100 cycles per step, 20 cycles for the transition between two excitation frequency steps, and an excitation level of 0.2 g; while, Fig. 12(b) presents the displacement for a case in the pre-buckling state at 5°C, where the excitation step size was 2 Hz, with 1000 cycles per step.

As shown in Fig. 13, the first test was conducted at 5°C (green curve), where the beam remained in its pre-buckling state, in this case the beam is subjected to axial tension as the temperature is lower than the reference. In this condition, the structure exhibited a hardening-type nonlinearity, characterized by an increase in effective stiffness with amplitude, which shifts the resonance peak upward, see Table 4. As the temperature increased to 30°C (blue curve), the nonlinear behavior became more pronounced, with stronger curvature in the amplitude-frequency response. At approximately 35°C (gray curve), the system reached a critical transition point, marking the onset of buckling. Beyond this temperature, the beam enters in the post-buckling regime. This is evident at 37.5°C (pink curve), where the response reverts to a softening behavior. With a further temperature increase, the response became increasingly nonlinear, as shown in the brown curve with a temperature of 48°C, reflecting the complex interplay between geometric nonlinearity and thermal effects in the post-buckling state. It is worth to mention that at the pre-buckling regime, where the dynamic response changes smoothly with frequency, a larger frequency step, i.e. 2 Hz, is sufficient to characterize the system without losing significant information. As the temperature increases and the beam enters the post-buckling regime, smaller step, i.e. 0.1 Hz, is required to capture the nonlinear variations in the response.

The dynamic nonlinear behaviour of the beam—particularly in the post-buckling states—is presented in Fig. 13 by considering the temperature tolerance of the climate chamber. Although the theoretical backbone approaches one, the experimental tests conducted in the climate chamber (with a tolerance of ±1°C) bring measurement tolerances in the measured natural frequency. As a result, the trend of the backbone curve that is obtained from the tests nearly reach one remaining close within the tolerances, depending on the sensitivity of the system to temperature variations. Besides, the flexibility of the

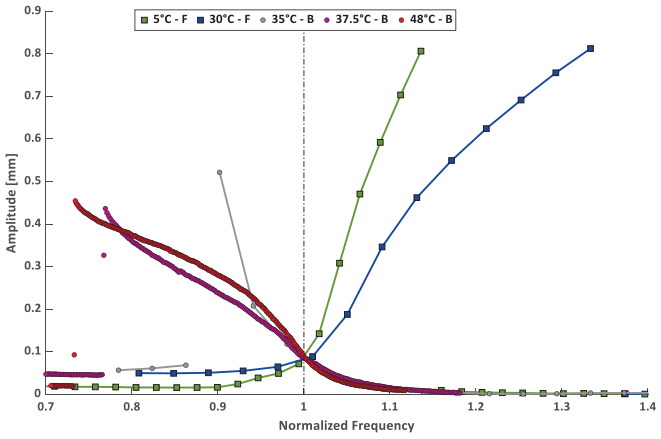

Fig. 13. Amplitude-frequency diagram regarding temperature from 5°C to 48°C (bi-metallic beam), Backward test: point symbol; Forward test: square symbol.

boundary conditions, which alters the effective stiffness and energy dissipation of the structure, produces small discrepancies between theory and experiment, as reported in Refs. [60,61]. The same analysis is conducted for the uniform aluminium beam as shown in Fig. 14. The test is carried out at two different temperatures of −10°C and +25°C; indeed, at low temperature the system is hardening and at higher temperature is softening. Therefore, to consider just the higher branch of amplitude-frequency diagram, a forward test is carried out at −10°C and a backward test is carried out at 25°C.

To have a better analysis, time history response and FFT spectra are presented in Fig. 15 and Fig. 16, for two different cases: one in pre-buckling and one post-buckling states during both forward and backward test.

Fig. 17 illustrates the influence of excitation strategy and excitation energy on the nonlinear dynamic response of the bi-metallic beam at two representative thermal conditions, corresponding to pre-buckling (10°C) and post-buckling (48°C) states. The purpose of this figure is not to directly compare the two thermal states, but rather to highlight how different excitation approaches and their level of excitation affect the measured dynamics depending on the underlying thermo-mechanical regime of the system.

In the pre-buckling condition, two excitation strategies are considered: constant acceleration levels: 1.5 g and 0.1 g (Fig. 17-a-II: brown and blue colors respectively), and constant voltage inputs: 0.01 V, 0.05

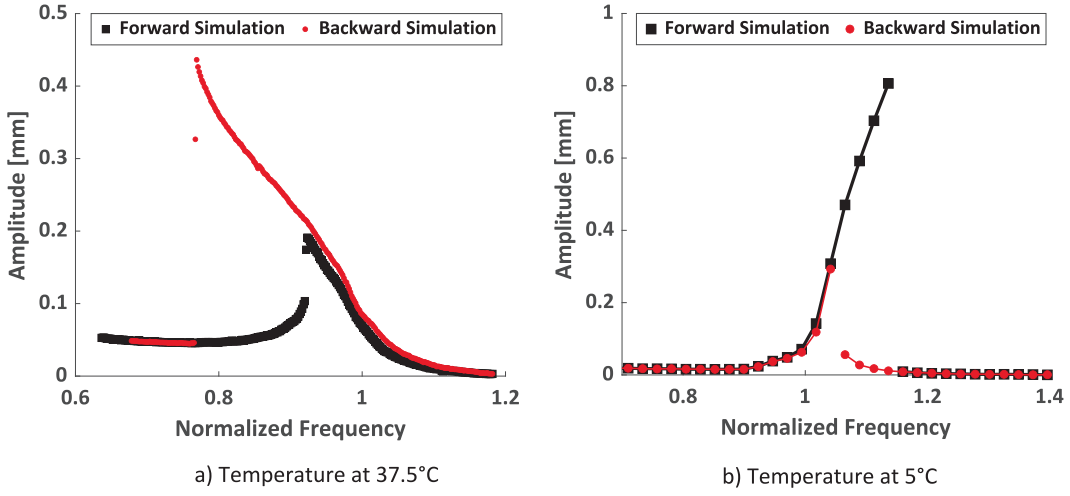

Fig. 12. Amplitude-frequency diagram of the bi-metallic beam regarding temperature for 37.5°C (a) and 5°C (b), Backward test: • red color; Forward test: ●black color.

Table 4
Identification of the jump phenomenon.

Forward test			Backward test		
Temperature [°C]	Amplitude [mm]	Frequency [ω/ω_n]	Temperature [°C]	Amplitude [mm]	Frequency [ω/ω_n]
5	0.806	1.103	5	0.056	1.034
30	0.812	1.347	30	0.041	1.143
35	0.209	0.96	35	0.521	0.92
37.5	0.191	0.861	37.5	0.436	0.716
48	0.197	0.909	48	0.454	0.717

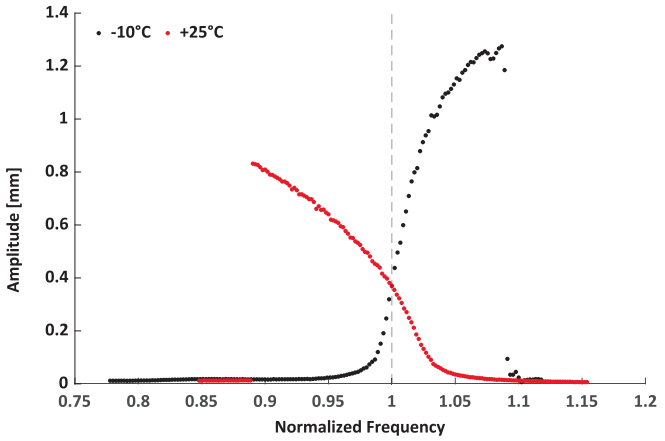

Fig. 14. Amplitude-frequency diagram regarding temperature at −10°C and 25°C for the uniform Al beam, Backward test at 25°C: • red points; Forward test at −10°C: ● black points.

V, and 0.1 V (Fig. 17-a-I: orange, green, and purple colors respectively). The resulting amplitude–frequency responses show comparable trends for both excitation approaches, with increasing excitation energy leading to larger vibration amplitudes. This similarity indicates that the choice of excitation strategy does not significantly alter the qualitative dynamic behavior of the system. Based on this observation, only the constant-acceleration excitation strategy is adopted in the post-buckling condition at 48°C. In the post-buckling condition at 48°C, the system displays strong sensitivity to excitation level and stability limits. Increasing the excitation level from 0.2 g to 0.4 g, Fig. 17-b: blue and brown colors respectively, does not result in a monotonic increase of the steady-state vibration amplitude; instead, the higher excitation drives the system into an unstable regime in which the buckled beam intermittently switches between coexisting equilibrium configurations.

To investigate more in-depth the behavior of the bi-metallic beam, a further test is conducted, where the beam is re-setup in the climate chamber on the shaker table. An FRF analysis is conducted to determine the accurate critical temperature, where there is a shift from hardening to softening. The FRF analysis bring us to 30°C as the critical temperature. Fig. 18 illustrates the amplitude–frequency response of the bi-metallic beam measured at the thermal condition of 30°C, corresponding to the onset of thermal buckling. The presented results were obtained by performing forward and backward frequency-sweep tests, plotted respectively as red (forward) and black (backward) markers. The two curves form a pronounced hysteretic loop, revealing the strongly nonlinear nature of the system in the vicinity of the buckling transition.

During the backward test, as the excitation frequency reduced from 60 Hz, the vibration amplitude rises gradually and then sharply at 46.2 Hz, where a sudden jump to a high-amplitude branch occurs. This jump represents a dynamic instability produced by the coexistence of multiple steady-state solutions. In this region, i.e., [46.2–60 Hz], the resonance peak bends toward lower frequencies, a signature of softening nonlinearity. The softening behavior arises because, above the buckling point, the beam is subjected to compressive thermal stresses that effectively reduce its bending stiffness. As the oscillation amplitude grows, these compressive stresses dominate the restoring force, causing the effective stiffness to decrease and the resonance frequency to shift leftward on the frequency axis. This phenomenon indicates that the beam is vibrating around a nearly straight post-buckled configuration weakened by thermal compression. Beyond this softening regime, as the excitation frequency continues to reduce beyond 46.2 Hz, the response progressively changes character, until the excitation frequency reaches 44.9 Hz, where we see a jump down. The amplitude of vibration no longer rises with frequency but begins to level off, and the slope of the curve reverses direction, bending toward higher frequencies. This marks the emergence of a hardening regime. The hardening regime becomes completed by conducting the forward sweep test, where the response of the system experienced a jump up at 46.7 Hz. The hardening behavior is observed till the excitation frequency reaches 69.9 Hz.

Physically, once the beam crosses the buckling threshold during vibration, it oscillates about a deflected post-buckled equilibrium shape. In this state, mid-plane stretching, residual tension in the outer layers, and geometric curvature effects generate additional restoring forces that counteract the earlier softening trend. The resulting geometric stiffening shifts the resonance peak toward higher frequencies, giving rise to the observed hardening branch. The coexistence of both softening and hardening regions within a single temperature condition demonstrates that the beam operates precisely at the boundary between pre- and post-buckling states. This mixed nonlinear response, seldom captured experimentally, provides direct evidence of the dynamic coupling between thermal loading, and geometric nonlinearity in bi-metallic structures.

4. Conclusion

This work presents an experimental investigation of the thermo-mechanical dynamic behavior of a bi-metallic beam made of aluminum and copper layers joined by explosive welding. Residual stresses were relieved by post-weld heat treatment; also, microstructural inspection and tensile tests confirmed interface integrity without delamination. The study examines nonlinear vibration and thermal buckling under controlled conditions, focusing on the transition between pre- and post-buckling regimes. Unlike mainly numerical or static studies, this work provides experimental evidence of thermal-dependent nonlinear dynamics in layered metallic structures. Random tests in a climatic chamber showed a non-monotonic change in the fundamental natural frequency. As temperature increased from 5°C to about 30°C, the first natural frequency decreased by nearly 32%, indicating thermal buckling onset. Above this temperature, the frequency increased due to geometric stiffening in the post-buckled state. The damping ratio showed the opposite trend, rising from 1.12% at 5°C to 3.51% at 35°C, demonstrating strong coupling between thermal loading, geometric nonlinearity, and energy dissipation.

A comparative study on a homogeneous aluminum beam under similar conditions clarified the role of nonlinear geometry. The uniform beam showed smoother thermal effects mainly governed by uniform axial stress, while the bi-metallic beam exhibited stronger nonlinear

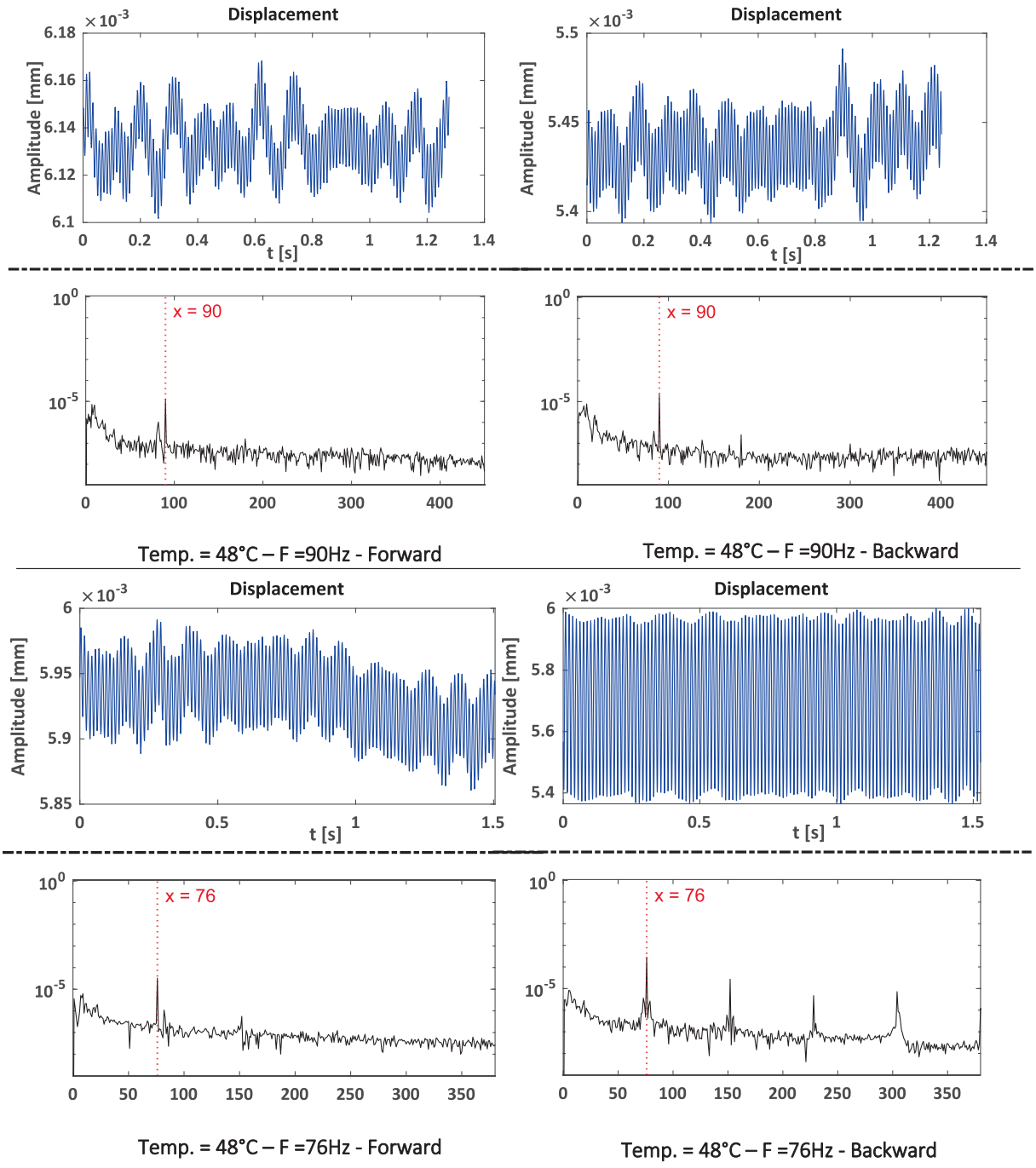

Fig. 15. Time history responses and FFT spectra of case in post-buckling state (at 48°C) at two: 90 Hz and 76 Hz, excitation frequencies (bi-metallic beam).

behavior due to differential thermal expansion and residual curvature. For the aluminum beam, the first natural frequency gradually decreased with temperature, reached a minimum near the transition between tensile and compressive axial states, then increased, forming a U-shaped trend. Its damping ratio increased slightly near this transition and remained low elsewhere, indicating weak nonlinearity. In contrast, the bi-metallic beam showed a sharper frequency drop before buckling and a stronger recovery after the critical temperature, reflecting enhanced geometric stiffening from thermally induced bending and material mismatch. Damping amplification near instability was also stronger in the case of bimetallic beam, indicating greater energy dissipation from nonlinear deformation and interface effects. Overall, the uniform beam response was mainly controlled by uniform thermal stress and modulus variation, while the bi-metallic beam exhibited stronger nonlinear dynamics driven by coupled axial and bending effects from material heterogeneity.

Stepped-sine tests further examined thermal-dependent nonlinear behavior across pre-buckling, near-critical, and post-buckling regimes. Forward and backward sweeps revealed amplitude-dependent dynamics. In the pre-buckling regime, axial tension produced hardening behavior, with resonance peaks shifting to higher frequencies as the excitation increased. Near the critical temperature, nonlinearity intensified and transitioned. In the post-buckling regime, the response shifted to softening with stronger nonlinear effects dominated by geometric nonlinearity and thermally induced bending.

A major contribution of this paper is the experimental identification of softening-to-hardening transitions near the critical temperature. Stepped-sine tests revealed coexisting softening and hardening

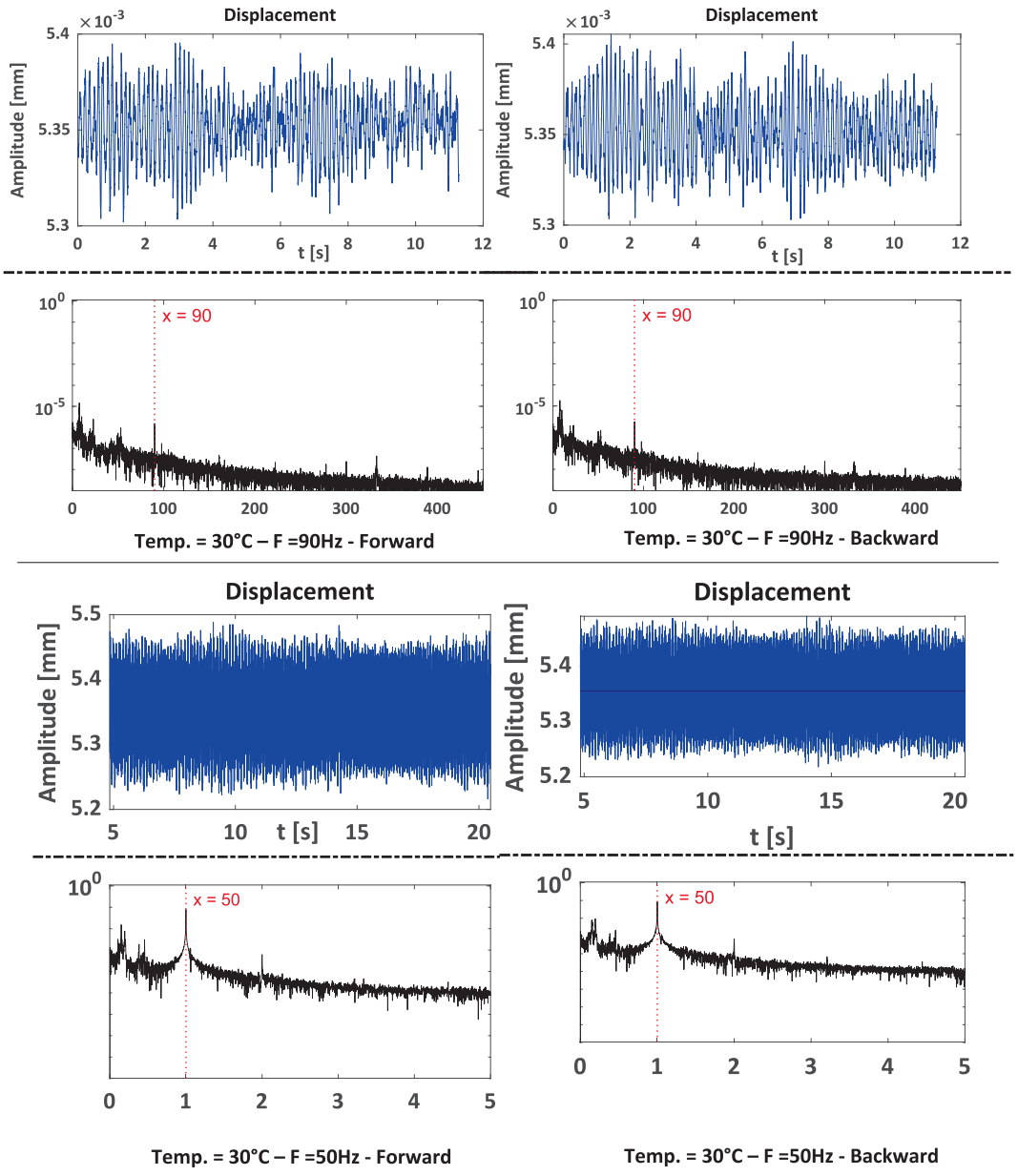

Fig. 16. Time history responses and FFT spectra of case in pre-buckling state (at 30°C) at two: 90 Hz and 50 Hz, excitation frequencies (bi-metallic beam).

nonlinearities at the buckling threshold, with clear hysteresis and jump phenomena. At 30°C, forward and backward sweeps showed strong hysteresis. During the backward sweep, a jump to a high-amplitude branch occurred around 46.2 Hz with resonance bending toward lower frequencies, indicating softening due to thermally induced compressive stresses. As frequency decreased, the response shifted to hardening, with a jump-down near 44.9 Hz. The forward sweep completed the hardening branch, with a jump-up around 46.7 Hz and stiffening at higher frequencies. The coexistence of softening and hardening at one temperature shows operation at the boundary between pre- and post-buckling states, where oscillations occur around a weakly deflected equilibrium. This provides experimental evidence of strong coupling between thermal loading and geometric nonlinearity.

Even though this study is focused on a detailed experimental analysis of specific bi-metallic beam under controlled thermal conditions and does not systematically examine geometric parameters, material combinations, it establishes a reliable experimental benchmark for thermo-mechanical nonlinear dynamics of bi-metallic structures in variable thermal environments. The temperature range of 5°C to 70°C was selected to ensure stable materials and repeatable measurements while clearly observing thermo-mechanically induced nonlinear phenomena. The results offer valuable physical insight and reference data for setting and validating numerical and theoretical models.

CRediT authorship contribution statement

Moslem Molaie: Writing – review & editing, Writing – original draft, Visualization, Software, Methodology, Investigation, Formal analysis, Data curation, Conceptualization. **Antonio Zippo:** Writing – review & editing, Writing – original draft, Visualization, Validation, Supervision, Software, Resources, Project administration, Methodology, Investigation, Funding acquisition, Formal analysis, Data curation, Conceptualization. **Emil Manoach:** Writing – review & editing, Writing – original draft, Methodology, Investigation, Funding acquisition, Formal analysis, Conceptualization. **Simona Doneva:** Writing – review & editing, Writing – original draft, Investigation, Conceptualization. **Jerzy Warminski:** Writing – review & editing, Writing – original draft, Methodology, Investigation, Funding acquisition, Formal analysis,

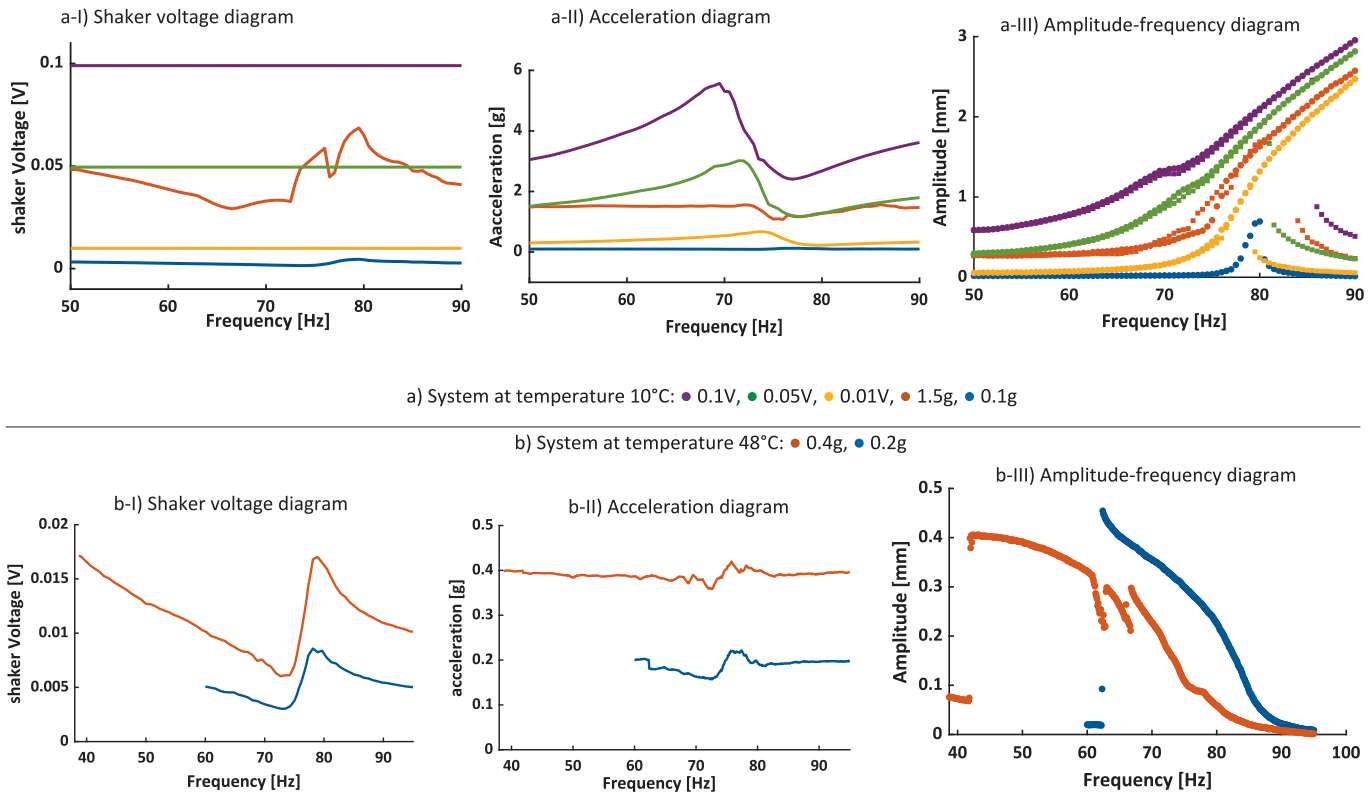

Fig. 17. Effect of excitation energy on dynamic responses at two: 10°C and 48°C temperatures (bi-metallic beam).

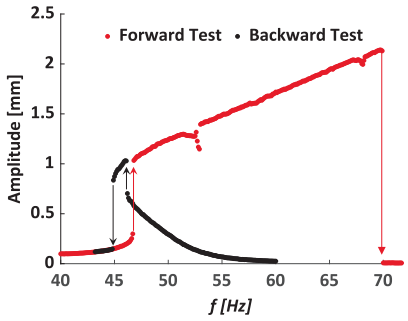

Fig. 18. Amplitude–frequency response of the bi-metallic beam at 30°C: transition between softening and hardening behavior, • forward test, ● backward test.

Conceptualization. **Francesco Pellicano:** Writing – review & editing, Writing – original draft, Visualization, Validation, Supervision, Resources, Project administration, Methodology, Investigation, Funding acquisition, Formal analysis, Data curation, Conceptualization.

Funding

This research was funded by NATO grant SPS program, grant number G6176 project title "Composite Metamaterials for Aerospace Structures – CoMetA".

Declaration of competing interest

The authors declare that they have no known competing financial interests or personal relationships that could have appeared to influence the work reported in this paper.

Acknowledgement

The fifth author acknowledge the support from Mechanical Engineering Discipline Grant M/FD-20/IM-5/129. The last (sixth) author acknowledge the funding support by NATO grant SPS program, project G6176 "Composite Metamaterials for Aerospace Structures – CoMetA". The third and fourth authors acknowledge the support obtained by Bulgarian research fund, grant KP-06-N72/7, 2023 and partial support by the Ministry of Education and Science – Bulgaria through Grant No. D01-98/26.06.2025.

Data availability

Data will be made available on request.

References

[1] Chroni E, Bakalakos S, Sotiropoulos G, Papadopoulos V. Topology optimization of bi-material structures with Iso-XFEM. Compos Struct 2024;1(331):117902. https://doi.org/10.1016/j.compstruct.2024.117902.
[2] Lu B, Zhang J, Zheng D, Shen C, Zhang T. A yield curve for bi-material structures and its application in energy absorption analysis of FML beam. Compos Struct 2023;15(312):116895. https://doi.org/10.1016/j.compstruct.2023.116895.
[3] Hajianmaleki M, Qatu MS. Vibrations of straight and curved composite beams: a review. Compos Struct 2013;1(100):218–32. https://doi.org/10.1016/j.compstruct.2013.01.001.
[4] Rehfield LW. Nonlinear free vibrations of elastic structures. Int J Solids Struct 1973;9(5):581–90. https://doi.org/10.1016/0020-7683(73)90071-1.
[5] Bennouna MM, White RG. The effects of large vibration amplitudes on the fundamental mode shape of a clamped-clamped uniform beam. J Sound Vib 1984;96(3):309–31. https://doi.org/10.1016/0022-460X(84)90359-6.
[6] Benamar R, Bennouna MMK, White RG. The effects of large vibration amplitudes on the mode shapes and natural frequencies of thin elastic structures part I: simply supported and clamped-clamped beams. J Sound Vib 1991;149(2):179–95. https://doi.org/10.1016/0022-460X(91)90630-3.
[7] Pellicano F, Mastroddi F. Nonlinear Dynamics of a Beam on Elastic Foundation. Nonlinear Dyn 1997;14(4):335–55. https://doi.org/10.1023/A:1008297721253.
[8] Pellicano F, Vestroni F. Nonlinear dynamics and bifurcations of an axially moving beam. J Vib Acoust 1999;122(1):21–30. https://doi.org/10.1115/1.568433.

[9] Pellicano F. On the dynamic properties of axially moving systems. J Sound Vib 2005;281(3):593–609. https://doi.org/10.1016/j.jsv.2004.01.029.

[10] Ma H, Ji W, Zhang H, Zhang Y, Lv S, Sun W. Nonlinear vibration of series-parallel fluid-conveying spatial-pipe systems with constrained-layer damping. Int J Mech Sci 2025;15(296):110334. https://doi.org/10.1016/j.ijmecsci.2025.110334.

[11] Tang Y, Zhong S, Yang T, Ding Q. Interaction between thermal field and two-dimensional functionally graded materials: a structural mechanical example. Int J Appl Mechanics 2019;11(10):1950099. https://doi.org/10.1142/S1758825119500996.

[12] Breslavsky D, Palamarchuk P, Tatarinova O, Altenbach H, Pellicano F. The influence of a sudden impact loading on the creep, damage, and fracture of beams made from functionally graded materials. Fat Fract Eng Mater Struct 2025;48(2):931–41. https://doi.org/10.1111/ffe.14528.

[13] Kurpa L, Pellicano F, Shmatko T, Zippo A. Free vibration analysis of porous functionally graded material plates with variable thickness on an elastic foundation using the R-functions method. Math Comput Appl 2024;29(1):10. https://doi.org/10.3390/mca29010010.

[14] Tahir SI, Chikh A, Tounsi A, Al-Osta MA, Al-Dulaijan SU, Al-Zahrani MM. Wave propagation analysis of a ceramic-metal functionally graded sandwich plate with different porosity distributions in a hygro-thermal environment. Compos Struct 2021;1(269):114030. https://doi.org/10.1016/j.compstruct.2021.114030.

[15] Arshid E, Khorasani M, Soleimani-Javid Z, Amir S, Tounsi A. Porosity-dependent vibration analysis of FG microplates embedded by polymeric nanocomposite patches considering hygrothermal effect via an innovative plate theory. Eng Comput 2022;38(5):4051–72. https://doi.org/10.1007/s00366-021-01382-y.

[16] Malekzadeh P, Shojaee A. Dynamic response of functionally graded beams under moving heat source. J Vib Control 2014;20(6):803–14. https://doi.org/10.1177/1077546312464990.

[17] Abramovich H, Govich D, Grunwald A. Buckling prediction of panels using the vibration correlation technique. Prog Aerospace Sci 2015;78:62–73. https://doi.org/10.1016/j.paerosci.2015.05.010. Special Issue: DAEDALOS - Dynamics in Aircraft Engineering Design and Analysis for Light Optimized Structures.

[18] Shahgholian-Ghahfarokhi D, Aghaei-Ruzbahani M, Rahimi G. Vibration correlation technique for the buckling load prediction of composite sandwich plates with isogrid cores. Thin-Walled Struct 2019;1(142):392–404. https://doi.org/10.1016/j.tws.2019.04.027.

[19] Kalnins K, Arbelo MA, Ozolins O, Skukis E, Castro SGP, Degenhardt R. Experimental nondestructive test for estimation of buckling load on unstiffened cylindrical shells using vibration correlation technique. Shock Vib 2015;2015(1):729684. https://doi.org/10.1155/2015/729684.

[20] Baciu TD, Franzoni F, Degenhardt R, Kalnins K, Bisagni C. Shape and loading imperfection sensitivity of the vibration-correlation technique for buckling analysis of cylindrical shells. Eng Struct 2024;1(304):117605. https://doi.org/10.1016/j.engstruct.2024.117605.

[21] Laureano M, da Silva A, Franzoni F, Carvalho Brito Jr. G. Vibration correlation technique: methodology applied to buckling of large-scale sandwich cylindrical shell. Lat Am Appl Res 2024. http://laar.plapiqui.edu.ar/OJS/index.php/laar/article/view/3337.

[22] Baciu TD, Franzoni F, Degenhardt R, Gliszczynski A, Bisagni C. Vibration-correlation technique for predicting the compressive buckling load of cylindrical shells under combined loading. Thin-Walled Struct 2025;1(216):113576. https://doi.org/10.1016/j.tws.2025.113576.

[23] Reddy JN. Mechanics of laminated composite plates and shells: theory and analysis. second edition. CRC Press; 2003. p. 864.

[24] Abramovich H. Stability and vibrations of thin-walled composite structures. Woodhead Publishing; 2017. p. 772.

[25] Franzoni F, Degenhardt R, Albus J, Arbelo MA. Vibration correlation technique for predicting the buckling load of imperfection-sensitive isotropic cylindrical shells: an analytical and numerical verification. Thin-Walled Struct 2019;1(140):236–47. https://doi.org/10.1016/j.tws.2019.03.041.

[26] Abramovich H. The Vibration Correlation Technique – a reliable nondestructive method to predict buckling loads of thin walled structures. Thin-Walled Struct 2021;1(159):107308. https://doi.org/10.1016/j.tws.2020.107308.

[27] Ravi JT, Nidhan S, Muthu N, Maiti SK. Analytical and experimental studies on detection of longitudinal, L and inverted T cracks in isotropic and bi-material beams based on changes in natural frequencies. Mech Syst Sig Process 2018;15(101):67–96. https://doi.org/10.1016/j.ymssp.2017.08.025.

[28] Wen SR, He XT, Chang H, Sun JY. A two-dimensional thermoelasticity solution for bimodular material beams under the combination action of thermal and mechanical loads. Mathematics 2021;9(13):1556. https://doi.org/10.3390/math9131556.

[29] Lin IK, Zhang X, Zhang Y. Thermomechanical behavior and microstructural evolution of SiN{sub x}/Al bimaterial microcantilevers. J Micromech Microeng Struct Dev Syst 2009;15:19. https://doi.org/10.1088/0960-1317/19/8/085010.

[30] Simonetti SK, Turkalj G, Banić D, Lanc D. Bimetallic thin-walled box beam thermal buckling response. Materials 2022;15(21):7537. https://doi.org/10.3390/ma15217537.

[31] Boley BA, Weiner JH. Theory of thermal stresses. New York, NY: John Wiley & Sons Inc; 1967. p. 586.

[32] Shang Y, Ye X, Feng J. Theoretical analysis and simulation of thermoelastic deformation of bimorph microbeams. Sci China Technol Sci 2013;56(7):1715–22. https://doi.org/10.1007/s11431-013-5217-2.

[33] Carpinteri A, Pugno N. Thermal loading in multi-layered and/or functionally graded materials: residual stress field, delamination, fatigue and related size effects. Int J Solids Struct 2006;43(3):828–41. https://doi.org/10.1016/j.ijsolstr.2005.05.009.

[34] Carpinteri A, Paggi M. Thermo-elastic mismatch in nonhomogeneous beams. J Eng Math 2008;61(2):371–84. https://doi.org/10.1007/s10665-008-9212-8.

[35] Srinivasan P, Spearing SM. Effect of heat transfer on materials selection for bimaterial electrothermal actuators. J Microelectromech Syst 2008;17(3):653–67. https://doi.org/10.1109/JMEMS.2008.918617.

[36] Wu GY. The analysis of dynamic instability of a bimaterial beam with alternating magnetic fields and thermal loads. J Sound Vib 2009;327(1):197–210. https://doi.org/10.1016/j.jsv.2009.06.012.

[37] Manoach E, Doneva S, Coupled WJ. Thermo-elastic large amplitude vibration of bi-material beams. Cham: Springer International Publishing; 2020. 10.1007/978-3-030-47491-1_13.

[38] Manoach E, Warminski J, Kloda L, Warminska A, Doneva S. Nonlinear vibrations of a bi-material beam under thermal and mechanical loadings. Mech Syst Sig Process 2022;1(177):109127. https://doi.org/10.1016/j.ymssp.2022.109127.

[39] Doneva S, Warminski J, Manoach E. Dynamic behaviour of two-layered beam subjected to mechanical load in thermal environment. Materials 2025;18(17):4167. https://doi.org/10.3390/ma18174167.

[40] Eltaher MA, Mohamed N, Mohamed SA, Seddek LF. Periodic and nonperiodic modes of postbuckling and nonlinear vibration of beams attached to nonlinear foundations. App Math Model 2019;1(75):414–45. https://doi.org/10.1016/j.apm.2019.05.026.

[41] Dong YH, Zhang YF, Li YH. An analytical formulation for postbuckling and buckling vibration of micro-scale laminated composite beams considering hygrothermal effect. Compos Struct 2017;15(170):11–25. https://doi.org/10.1016/j.compstruct.2017.02.093.

[42] Emam SA, Eltaher MA, Khater ME, Abdalla WS. Postbuckling and free vibration of multilayer imperfect nanobeams under a pre-stress load. Appl Sci 2018;8(11):2238. https://doi.org/10.3390/app8112238.

[43] Daneshkhah E. Analysis of Thin-Walled Beam and Flexible Plate Structures through the Unified Formulation. Italy; 2022. https://iris.polito.it/handle/11583/2972205.

[44] Pagani A, Augello R, Carrera E. Frequency and mode change in the large deflection and post-buckling of compact and thin-walled beams. J Sound Vib 2018;13(432):88–104. https://doi.org/10.1016/j.jsv.2018.06.024.

[45] Chakraborty S, Dey T, Jiang J, Amabili M. Influence of non-uniform temperature gradient on thermal post-buckling and vibration response of bi-directional functional graded composite plates. Compos Struct 2025;1(371):119526. https://doi.org/10.1016/j.compstruct.2025.119526.

[46] Chakraborty S, Dey T, Mahesh V, Harursampath D. Post-buckling and vibration analysis of randomly distributed CNT reinforced fibre composite plates under localised heating. Mech Adv Mater Struct 2023;30(21):4430–49. https://doi.org/10.1080/15376494.2022.2095470.

[47] Chakraborty S, Dey T, Kumar R. Stability and vibration analysis of CNT-Reinforced functionally graded laminated composite cylindrical shell panels using semi-analytical approach. Compos B Eng 2019;1(168):1–14. https://doi.org/10.1016/j.compositesb.2018.12.051.

[48] Chakraborty S, Dash S, Dey T. Non-linear stability characteristics of randomly distributed CNT-reinforced fiber composite beams under thermo-mechanical loadings. Mech Based Des Struct Mach 2024;52(9):7021–44. https://doi.org/10.1080/15397734.2023.2297240.

[49] Dash S, Chakraborty S, Dey T, Kumar R. Buckling and free vibration analysis of randomly distributed CNT reinforced composite beam under thermomechanical loading. Eur J Mech A Solids 2022;1(96):104749. https://doi.org/10.1016/j.euromechsol.2022.104749.

[50] Dash S, Dey T, Haldar A, Kumar R. A semi-analytical method for non-linear instability analysis of variable stiffness laminated composite beams under thermo-mechanical loading. Compos Struct 2025;1(357):118966. https://doi.org/10.1016/j.compstruct.2025.118966.

[51] Vosteen LF. Effect of temperature on dynamic modulus of elasticity of some structural alloys [Internet]. 1958 [cited 2026 Feb 18]. Available from: https://ntrs.nasa.gov/citations/19930085159.

[52] Glazer J, Morris JW, Kim SA, Austin MW, Ledbetter HM. Temperature variation of the elastic constants of aluminum alloy 2090-T81. AIAA J 1987;25(9):1271–2. https://doi.org/10.2514/3.9779.

[53] Pashchin MO, Shlonskyi PS, Bryzgalin AG, Kushnaryova OS, Todorovych NL. Features of formation of structure of coaxial joints of copper and aluminium in explosion welding with vacuuming of welding gap. Vol. 02. 2021;02:2–7. doi: https://doi.org/10.37434/tpwj2021.02.01.

[54] Dobrushin LD, Bryzgalin, AG, Shlonskiy PS, Pekar ED, Ventsev SD. Development of the technology of manufacturing hardware clamps, using explosion welding. 2021;41–6. doi: https://doi.org/10.37434/as2021.08.08.

[55] Shlyonskyi PS. Explosion welding of copperaluminium pipes by the “reverse scheme.” Vol. 08. 2020;08:51–3. doi: https://doi.org/10.37434/as2020.08.08.

[56] Corral Á. Universal finite-time scaling in the transcritical, saddle-node, and pitchfork discrete and continuous bifurcations. Chaos 2025;35(1):013106. https://doi.org/10.1063/5.0231950.

[57] Huang J, Su KLR, Lee YYR, Chen S. Various bifurcation phenomena in a nonlinear curved beam subjected to base harmonic excitation. Int J Bifurcation Chaos 2018. https://doi.org/10.1142/S0218127418300239. Located at: world.

[58] Wang Z, Meng Q. An analytical study on the thermal post-buckling behaviors of geometrically imperfect FRC-laminated beams using a modified zig-zag beam model. Aerospace 2025;12(2):138. https://doi.org/10.3390/aerospace12020138.

[59] Zheng HT, Ding H. Softening-hardening nonlinear dynamics of a beam with concentrated mass and axially elastic boundaries. Nonlinear Dyn 2025;113(20):27085–105. https://doi.org/10.1007/s11071-025-11583-5.
[60] Kloda L, Lenci S, Warminski J. Hardening vs. softening dichotomy of a hinged-simply supported beam with one end axial linear spring: experimental and numerical studies. Int J Mech Sci 2020;15(178):105588. https://doi.org/10.1016/j.ijmecsci.2020.105588.
[61] Kloda L, Lenci S, Warminski J. Nonlinear dynamics of a planar beam–spring system: analytical and numerical approaches. Nonlinear Dyn 2018;94(3):1721–38. https://doi.org/10.1007/s11071-018-4452-2.